A Multipurpose Micro-pulse Reactor for Studying Gas-phase Reactions

P. Zamostny,* Z. Belohlav, and L. Starkbaumova
Department of Organic Technology, Institute of Chemical Technology, Prague
Technická 5, 166 28 Praha 6, E-mail: petr.zamostny@vscht.cz

Original scientific paper
Received: April 18, 2006
Accepted: October 26, 2006

The article is focused on the aspects of using micro-catalytic pulse reactors for studying gas-phase reactions. A literature review includes data regarding different types of micro-catalytic pulse reactor applications in heterogeneous catalysis and the techniques used for estimating kinetic parameters are summarized. The experimental part describes the adaptation of a pyrolysis chromatograph to a micro-catalytic reactor. The mathematical model of a homogeneous pulse carried by the carrier-gas in the plug-flow regime is developed and the assumptions regarding its validity are tested on a model reaction. Three examples describing the application of the technique to non-catalyzed reaction system screening, catalyst screening, and kinetic data measurement followed by estimation of the kinetic quantities of the model reaction by non-linear regression are provided in the article.

Key words:
Micro-pulse reactor, reaction kinetics, selectivity

Introduction

Due to the discontinuous character of their operation allowing a direct link between the reaction and the analytical part of an apparatus, pulse reactors occupy an interesting position among all those used for studying different aspects of chemical reactions in the gaseous phase. Their concept was published as early as in the mid 20th century[1] but their more intensive application was postponed until the last two decades, when sophisticated and cheap GC and GC-MS methods appeared. Pulse reactors are often called micro-pulse or micro-catalytic pulse reactors as they work well with much smaller amounts of reaction mixture and/or catalyst than most other laboratory reactors. The direct link between the reaction and the analytical parts, and the absence of sample manual manipulation contribute to measurement precision and reproducibility, as well as to the ease of operation. Micro-pulse reactors thus enable to carry out many experiments in relatively short time-frame.

A micro-pulse reactor is usually implemented by a plug-flow tube reactor, flowed by the stream of an inert medium, equipped with a sampling device enabling the pulse of a reaction mixture to be inserted into the flowing medium stream. Optionally, a catalyst bed can be placed inside the reactor tube. This possibility represents no significant construction change, and catalyst and inert beds can be readily swapped thus allowing the comparison of a catalytic and non-catalytic reaction in an identical environment. The reactor tube is usually placed in an oven controlling the reactor temperature or the temperature is controlled by other means. The components of the reaction mixture react while they pass through the heated zone or the catalyst bed. The reaction products are carried into the analytical part (usually gas-chromatograph) where the composition of the final reaction mixture is detected.

A majority of published papers reference the use of liquid sample volume between 0.1 and 5 μl. Micro-reactors are usually made of quartz or stainless steel. Their inner diameter rarely exceeds 10 mm in order to ensure a negligible radial temperature profile within the reactor heated by an electric furnace. The temperature in the hot-zone is generally a function of both the outer wall temperature and the flow rate of the carrier gas. Therefore, the temperature must be measured directly in the reactor or other means for determining its actual value must be present. The sample residence time in the hot-zone of the reactor can be altered by changing the carrier gas flow rate, provided that the pressure inside the reactor is constant. Micro-catalytic reactors also provide another option – changeable length of the catalyst bed – which is however more difficult and time-consuming. The important characteristics of the micro-catalytic pulse reactor are also the short contact time between the sample and the catalyst causing only very small deactivation of the catalyst.

Micro-pulse reactors are frequently used for catalyst screening. The representative examples of their applications, summarized in Table 1, are often aimed at the investigation of catalyst activity and/or

*Corresponding author

selectivity based on the composition of the reaction mixture. Thus, there are many studies, such as those of *Igarashi* and *Ogino*[2] and *Campelo* et al.,[3] which employed the micro-pulse reactor for measuring the conversion and selectivity of various reaction systems.

On the other hand, there are also studies that intend using measured data for kinetics modelling and they are aimed at better definition of experimental conditions in the pulse reactor. The work of *Susu* and *Ako*,[7] who studied ethylbenzene isomerization on bifunctional Pt/Al_2O_3 catalyst, can be considered a prime example. They studied the dependence of conversion and product yields on the reaction temperature and contact time, and offered a semi-quantitative analysis of the results. The study of the pulse size effect on the conversion was also performed, leading to the conclusion that conversion increases in proportion to pulse size. Therefore, during further experiments the authors maintained the pulse size of 1 μl to ensure data reliability. The same authors also used their technique for other reaction systems, e.g. *n*-octane dehydrocyclization.[9] *Ayo* and *Susu*[12] used slightly modified equipment for studying C_6-ring hydrogenation and dehydrogenation. In this work, they also studied the reaction mechanism quite successfully and tried to fit the experimental data using linear regression.

T a b l e 1 – *Overview of micro-pulse reactor applications for studying gas-phase chemical reactions*

Reactor	Reaction	Study focus	Feed	Ref.
Quartz d = 8 mm	ammonia and methanol synthesis	catalyst activity	gaseous, sampling loop	2
Quartz d = 8 mm	coal gassification	catalyst activity	solid	2
Quartz d = 8 mm	ethylene hydratation	catalyst activity	gaseous, sampling loop	2
Quartz d = 4 mm	n-dodecane hydrotreatment	catalyst screening	liquid, 0.5 – 5 μl	3
Stainless steel d = 4 mm	n-heptane reforming	influencing kinetics by operating conditions, deactivation	liquid, 1 μl	4
Stainless steel d = 4 mm	methylcyklohexane dehydrogenation and hydrogenolysis	influencing kinetics by operating conditions	liquid, 1 μl	5
Stainless steel d = 4 mm	3-methylhexane aromatization and dehydrogenation	influencing kinetics by operating conditions	liquid, 1 μl	5
Stainless steel d = 4 mm	hept-2-ene aromatization	influencing kinetics by operating conditions	liquid, 1 μl	6
Stainless steel d = 6.4 mm	ethylbenzene isomerization	reaction kinetics	liquid, 0.1 – 2 μl	7
Quartz d > 0.8 mm	cracking reactions	reaction kinetics	liquid, 1 μl	8
Stainless steel d = 6.4 mm	n-octane dehydrocyclization	catalyst screening	liquid, 0.1 – 2 μl	9
Iconel 600 (alloy) d = not listed	n-hexadecane catalytic cracking	reaction kinetics	gaseous, sampling loop	10
Glass d = 2.4 mm	n-hexane isomerization and cracking	reaction kinetics	liquid, 0.3 μl	11
Stainless steel d = 6.1mm	cyclohexane dehydrogenation	reaction kinetics and mechanism	liquid	12
Stainless steel d = 6.1mm	benzene hydrogenation	reaction kinetics and mechanism	liquid	12
Stainless steel d = 6.1mm	cyclohexane dehydrogenation/ benzene hydrogenation	reaction kinetics and mechanism	liquid	12
Pyrex glass d = 4 mm	benzene hydrogenation	reaction kinetics	gaseous, liquid, 1–10 μl	13

The agreement between their data and the model was only moderately good. Their work was further followed by *Aberuagba* and *Susu*[4,5] and *Aberuagba*[6] who studied the effect of the carrier gas on hydrocarbon reforming reactions, and also the process of deactivation, but the technique used for data processing and interpretation was not fundamentally different from the previous works.

Christoffel et al.[11] worked with a similar reaction system (isomerization and cracking of hexane isomers on a Pt/Al_2O_3 catalyst) and unlike the previous authors they observed no effect of pulse size on the conversions of both reactions. The difference can be probably explained by a different magnitude of sample sizes used in those studies (see Table 1 for comparison).

Sica et al.[13] used a glass micro-pulse reactor to perform the kinetic study of benzene hydrogenation. They paid special attention to the sampling procedure as they compared the results obtained by direct injection of the liquid sample by a micro-syringe with those obtained using a gas saturator sample valve device. They concluded that both methods produced similar Gaussian pulses and thus the former was chosen for practice due to its simplicity. The work also included fitting the measured data using a mathematical model. The authors derived both the power-law and the Langmuir-Hinshelwood models. In their models they used the triangular approximation of the pulse shape which corresponded quite well to the actual pulse profile they measured. However, the need to describe the pulse shape added significantly to model complexity and required experimental characterization of the pulse shape.

All previous indications, and according to Table 1, lead to the conclusion that cracking or elimination reactions of liquid reactants are the primary object of this technique, since the initial mixture can be easily created before it is carried into the reactor. Papers describing the use of pulse reactors for addition reactions or those working with educts in different phases are rare as they require an evaporator and a sampling loop,[2,10] unless the gas phase is used as the carrier gas. Although the direct introduction of a liquid sample into the reactor by the micro-syringe is very appealing due to its simplicity and thus it is preferred by most authors, it is also very sensitive to the implementation and may have a substantial (systematic) impact on the experimental data. While in certain types of studies, e. g. relative comparison of multiple catalysts or substrates, selectivity dependence on conversion, etc., the systematic error may represent only a minor problem as long as the reaction conditions are constant for all compared samples, it is very significant for any thorough tests that include the estimation of kinetic parameters. Although the monitoring and modelling of the pulse shape proposed by *Sica*[13] can be applied, the added difficulty is a big drawback for practical use. The main advantage of micro-pulse reactors is their simplicity and rapid operation and therefore, from the practical point of view, it can be still seen as a challenge to optimize the experimental setup so that the measured data would be ready for direct processing using similar techniques and models as in common flow reactors. The aim of this paper is to describe the development of such a reactor using commercially available equipment.

Experimental setup

Apparatus

A commercial apparatus for pyrolysis chromatography (Pyr-GC) was converted into the micro-pulse reactor with an on-line sample analysis. The apparatus is schematically shown in Fig. 1. The reactor part consists of a Shimadzu PYR-4A pyrolyser connected with the analytical part based on Shimadzu GC-17A gas chromatographs.

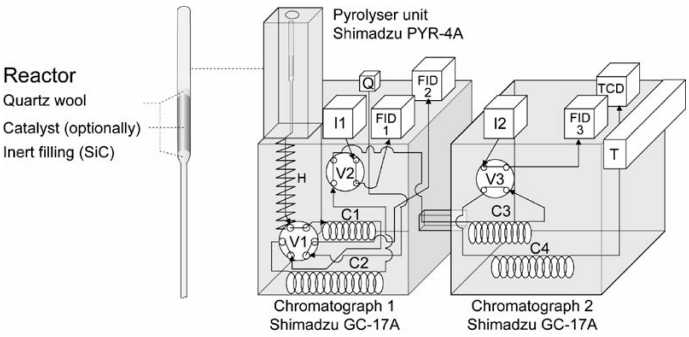

Fig. 1 – *Diagram of the micro-pulse reactor apparatus. – C1-C4: capillary columns, V1-V3: changeover valves, I1-I2: injectors, FID1-FID3: flame ionization detectors, TCD: thermal conductivity detector, Q: carrier gas source, H: additional heating, T: reactor temperature control.*

The micro-reactor, placed in the pyrolyser, is made of a quartz tube with a contraction in the middle (see Fig. 1). The length of the reactor is L = 195 mm, its inner diameters are D_i = 3 and D_i = 1 mm at the top and bottom parts respectively. The reactor is heated by an electric furnace and the temperature control allows setting up the temperature of the reactor outer wall. In all experimental setups, inert filling – consisting of carbide silica particles layered upon the plug of quartz wool – was placed into the reactor hot-zone. It was verified that the inert filling has multiple positive effects including quicker heating and evaporation of the sample and attaining uniform flow distribution of the reaction gas through the reactor. Its thermal capacity also

contributes to the stable temperature of the reactor. If the studied reaction involves a catalyst, it is inserted between the quartz wool and the carbide silica parts of the inert filling.

The original apparatus did not fulfill the needs for precise measurement of the flow rate through the reactor tube. It was remedied by implementing a mass flow meter in the carrier gas inlet to the reactor. The temperature in the hot-zone of the reactor or in the catalyst bed depended on not only the directly measured temperature of the outer reactor wall but also on the flow rate of the carrier gas. Direct measurement of the hot-zone temperature was possible, but such measurement was cumbersome during experiments. Therefore, a series of measurements of hot-zone temperature in relation to the outer wall temperature and the flow rate was made prior to the experiments. The measured data allowed determining the reaction temperature indirectly from the measured wall temperature and flow rate in further experiments.

Analytical methods

The analytical part of the apparatus was based on two connected gas chromatography units (2 × Shimadzu GC 17A). The gas chromatographic analysis of the reaction mixture was carried out in up to four capillary columns (for details see Tab. 2 and 3) switched by three changeover valves (Fig. 1). Three flame-ionization detectors and one thermal conductivity detector were available for detection.

Table 2 – *Reactor operating quantities*

Quantities	Specification
Temperature:	max. 820 °C
Pressure:	150–500 kPa
Carrier gas flow rate:	10–400 ml min^{-1}
Carrier gas:	1 gas or mixture of 2 gases
Sample state:	liquid, gaseous

Table 3 – *Capillary columns*

Column	Description
C1	Agilent DB-1, l = 10 m, d_i = 0.53 mm, δ = 1 μm film
C2	Agilent DB-1, l = 60 m, d_i = 0.32 mm, δ = 1 μm film
C3	Chrompack PLOT CP-Al2O3/KCl, l = 50 m, d_i = 0.32 mm, δ = 5 μm film
C4	Chrompack PLOT CP-Molsieve 5A, l = 15 m, d_i = 0.32 mm, δ = 30 μm film

The combination of two chromatograph ovens was necessary to attain different temperature programs in the different branches of the analytical path. A short deactivated column used as interface between the reaction and the analytical part was heated at least to 250 °C regardless of the GC temperature program to ensure quick and uniform transfer of the sample into the first column. Fig. 2 demonstrates the arrangement of the analytical path and its changes throughout the analysis. Each column represents an independent analytical section that can be connected to other sections by changeover valves. Basically, each column can be connected either to a subsequent column or to a detector. The connection is switched by electronically controlled valves. The initial setting arranges all columns in a series terminated by the TCD. The mixture can be split into up to four fractions, each being separated in one column. Fast eluents, such as hydrogen, pass all four columns while very slow ones pass only the first column. Unlike all the others, the C1 column is connected in reverse direction compared to the original arrangement. Therefore, all slowly eluting components are eluted in relatively close retention times in this column and, even more importantly, it ensures that all components will elute before the end of the analytical run.

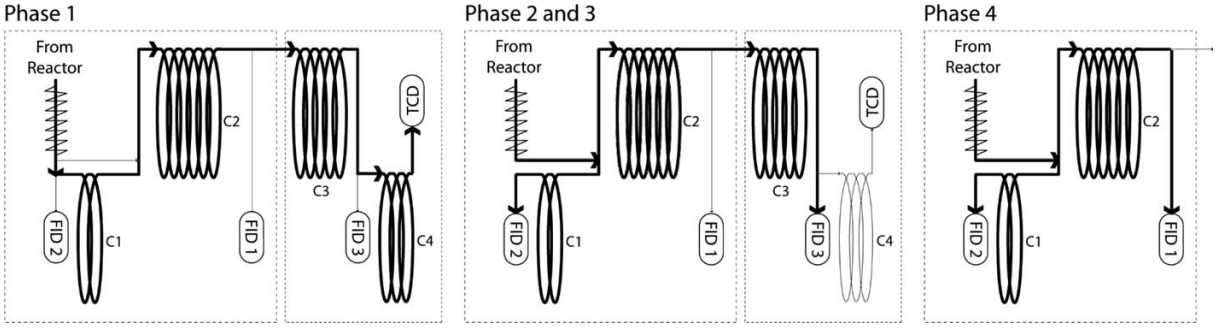

Fig. 2 – *Analysis operation flowchart. Phase 1 – Initial settings. Phase 2–3 – Detection of pyrolysis gases and oils. Phase 4 – Detection of pyrolysis gasoline.*

Sampling method

A chromatographic micro-syringe is typically used for injecting gaseous and liquid feedstock, while solid feedstock is introduced into the pyrolysis reactor by a platinum sample bucket when the Pyr-4A apparatus is operated. However, the technique of introducing the sample into the reactor had to be unified to achieve reproducible results for the different types of feedstock. Therefore, all sample types, including those having a higher melting point than the laboratory temperature (e. g. hydrocracking vacuum distillates) were introduced by the chromatographic syringe technique in either liquid or gaseous phase. The size of a liquid sample was very important for achieving consistent results. The analysis presented in our earlier work[17] has shown that the conversion of hydrocarbon by thermal cracking was independent of sample size in the range 0.1 – 0.5 μl, decreased slightly in range 0.5 – 0.8 μl, and decreased significantly above 0.8 μl. Decreased conversion in the case of larger injected volumes was caused by thermal effects of sample evaporation and reaction and by shortening the residence time due to thermal expansion of the sample. Therefore, the sample volumes above 0.5 μl had to be avoided to ensure data reliability. Samples also had to be injected in the immediate vicinity of the inert filling upper boundary to prevent the sample from sticking to the reactor wall in the colder zone. A micro-syringe equipped with a long needle (at least 9 cm) and able to inject low-volume samples in a reproducible way was necessary to fulfill the above-mentioned requirements. The dead-volume-free syringe Hamilton 7000.5 best accommodated the requirements, achieving deviations of the injected sample volume less than 5 %. The standard sample volume used in further experiments was 0.2 μl, which represented a good compromise between the low sample volume and its accuracy.

Mathematical modelling

The mathematical model uses the concept of a homogeneous pulse carried by the carrier-gas in the plug-flow regime, based on the following assumptions:

– The sampling technique produces an homogeneous rectangular pulse of the sample into the carrier-gas stream (i. e. the composition is constant throughout the whole pulse),

– The pulse retains its homogeneity as it passes through the reactor,

– The pulse flows through the reactor in the plug-flow regime, i. e.,

– The mass exchange does not occur between the pulse and the carrier gas.

Fulfilling the assumptions above, the reaction within the pulse runs under conditions identical to those in a continuous plug-flow reactor. Thus, the equivalent feed rate of the reaction mixture in the continuous reactor corresponding to the pulse reactor (Q_{pe}) is equal to the carrier-gas feed rate (Q_n)

$$Q_{pe} = Q_n \tag{1}$$

For non-catalyzed reactions the crucial parameter determining the conversion in the reactor is the equivalent residence time τ_r

$$\tau_r = \frac{V_r}{Q_{pe}} = \frac{V_r}{Q_n} \tag{2a}$$

where V_r is the reaction volume; while for heterogeneously catalyzed reactions it is the equivalent contact time

$$\frac{m_{cat}}{Q_{pe}} = \frac{m_{cat}}{Q_n} \tag{2b}$$

where m_{cat} is the total mass of the catalyst in the reactor. Since the pulse passes the reactor as a homogeneous segment with the rate of the carrier gas flow, the contact time is independent of the pulse size but depends solely on the carrier-gas feed rate, assuming a constant mass of the catalyst in the reactor. Hence the contact time can be altered by changing the carrier-gas feed rate.

Evaluating catalyst activity

Information about the pulse composition after the micro-pulse reactor related to the known composition of an injected pulse is the desired result of the experiment. A conversion of the key component can be calculated from obtained concentration data. The simplest way of evaluating catalyst activity is based on the comparison of key component conversions on different catalysts, without the rate equation and rate coefficients being determined. The relative comparison of activity is performed and is based on the mutual relation of contact times needed to attain certain conversion for each of the compared catalysts.

$$\frac{k_1}{k_2} = \frac{Q_{n1}}{Q_{n2}}, \quad X_1 = X_2 \tag{3}$$

where k is the rate coefficient and X is the key component conversion.

Evaluating catalyst selectivity

Evaluating selectivity of the process carried out on different catalysts is aimed at comparing the amount of undesired by-products. Having the selectivity of the process dependent on the conversion of the key component, the comparison must be based on a constant conversion level.

The evaluation of selectivity is sensitive to the validity of 'the homogeneous pulse carried by the carrier-gas in plug-flow regime' assumption. In addition, the concentration structure of the pulse must be independent of the carrier-gas feed rate. It can be accomplished if the pulse is not mixed with the carrier gas but inserted into the carrier-gas stream. High length of the pulse compared to the reactor diameter can promote such behaviour.

Estimating kinetic parameters from the pulse reactor data

The pulse reactor can be approximated with a model of an equivalent continuous reactor in steady state under the assumptions stated in the previous section. The equivalent continuous reactor is a plug-flow reactor operated with the equivalent residence or contact time given by eq. (2), at identical temperature and pressure. The reactor can be modelled as a plug-flow reactor under such approximation. The material balance of *i*-th component is thus given by eq. (4)

$$Q_{\mathrm{pe}} c_i + r_i \mathrm{d}V = Q_{\mathrm{pe}} (c_i + \mathrm{d}c_i) \tag{4a}$$

$$Q_{\mathrm{pe}} c_i + r_i \mathrm{d}m_{\mathrm{cat}} = Q_{\mathrm{pe}} [c_i + (\mathrm{d}c_i / \mathrm{d}m_{\mathrm{cat}}) \mathrm{d}m_{\mathrm{cat}}] \tag{4b}$$

where c_i is the concentration of the *i*-th component and r_i is the rate of its formation. The material balance is therefore a set of ODEs (5), the number of which is equal to the number of reaction components.

$$\frac{\mathrm{d}c_i}{\mathrm{d}\tau_{\mathrm{r}}} = r_i \tag{5a}$$

$$\frac{\mathrm{d}c_i}{\mathrm{d}(m_{\mathrm{cat}} / Q_{\mathrm{pe}})} = r_i \tag{5b}$$

The concentration can be computed from the ideal gas equation as

$$c_i = x_i \frac{p_{\mathrm{r}}}{R T_{\mathrm{r}}} \tag{6}$$

where X_i is the mole fraction of the *i*-th component in the mixture, R is the ideal gas constant, p_{r} is the reaction pressure, and T_{r} is the reaction temperature.

Results and discussion

Several examples studying non-catalyzed and heterogeneously catalyzed reaction systems were selected to demonstrate the validity of the employed mathematical model, the process of catalyst screening, and measuring kinetic data.

Studying the non-catalytic reaction system

Studying the thermal cracking reactions of hydrocarbon feedstock is one of the most typical applications of the pulse micro-reactor. Dodecane cracking was used as a model reaction to demonstrate the behaviour of the reaction system. The cracking reactions lead to a variety of reaction products, the most important being ethylene, propylene, methane, butenes, butadiene, and aromatics. The yields of the most important products at almost total conversion level are summarized in Fig. 3.

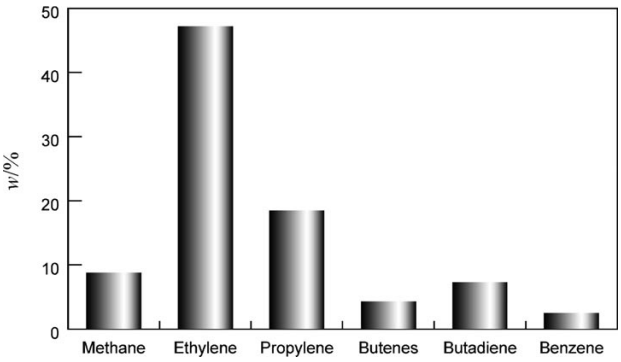

Fig. 3 – *Major products of dodecane thermal cracking at 800 °C (x ~ 1)*

Despite the fact that cracking dodecane involves quite a complex radical reaction mechanism comprising initiation, propagation, and termination steps, the existence of long reaction chains in the propagation phase make it resemble a simple reaction with the reaction rate corresponding to the rate-controlling step of hydrogen radical abstraction. Although more complex models are needed to describe the formation of reaction products, it was proved that the dodecane conversion can be well described by the first-order kinetics model.[14] Fig. 4 shows the conversion profiles measured at different temperatures in our pulse micro-reactor. The measured data were compared to the curves computed using the first-order kinetics model, the parameters of which were estimated by non-linear regression from the experimental data. Since there is good agreement between the measured data (which should follow the first-order kinetics) and the first-order model, it can be concluded that there are no significant adverse effects of evaporating sample or diluting the pulse by carrier gas, and therefore

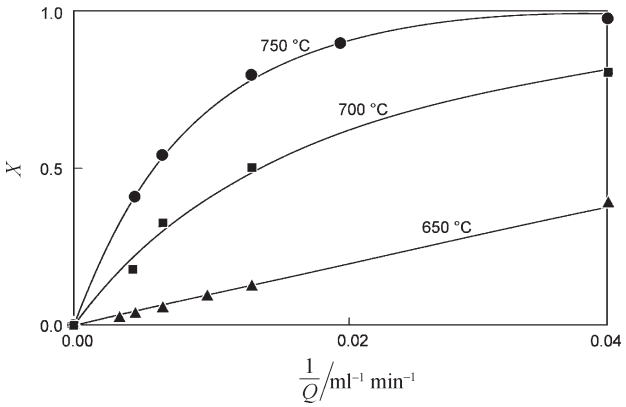

F i g . 4 – *Conversion of dodecane by thermal cracking at different temperatures. Point sizes reflect the expanded standard uncertainty at the 95 % level of confidence. Lines are computed by nonlinear regression using simplified 1st order kinetics model.*

the assumptions and the mathematical model proposed in section 3 can be justified.

Evaluating catalyst selectivity

Catalytic cracking of 1-hexene on catalyst EBK 13 (Chemopetrol Inc., CZ, w = 64 % zeolite ZSM-5 type) was used as a model reaction for evaluating the selectivity of the catalytic reaction. The catalyst bed was formed by 0.050 g of grinded catalyst extrudates of particle size 0.4–0.8 mm. Experiments were carried out at 500 °C and 300 kPa. The contact time was altered by changing the carrier gas (N_2) flow rate within the range 25 – 200 N ml min^{-1} and thereby the conversion also changed within 5 to 75 %. The conversion is calculated as transformation of 1-hexene to hydrocarbons with different numbers of carbon atoms. The isomerization of 1-hexene to other hexenes was not included into the conversion calculations.

The selectivity of cracking to most important products vs. conversion is plotted in Fig. 5. Selectivity to each product is expressed as the amount of formed product to the amount of converted 1-hexene. The cracking proceeds quite selectively to propylene, butenes, and ethylene (in that order) at lower conversion levels. It corresponds to the direct β-scission of the carbenium ion formed by interaction of 1-hexene double bond with the Brønsted acid site of the zeolite. Two isomers of carbenium ion can be formed. The β-scission of 2-hexyl carbenium ion leads ultimately to two molecules of propylene while that of 1-hexyl carbenium isomer gives an equimolar mixture of ethylene and butenes, which corresponds to roughly double butenes yield (mass) compared to ethylene observed at lower conversions. Since 2-hexyl carbenium ion is much more stable than 1-hexyl isomer, much higher yields of propylene were observed in comparison to those of ethylene and butenes. The dominance of direct β-scission diminishes at higher conversions where the carbocations become subjects of bimolecular oligomerization[15] in an increasing scale. Resulting intermediates can lead to a larger variety of products including those with more than six carbon atoms per molecule.

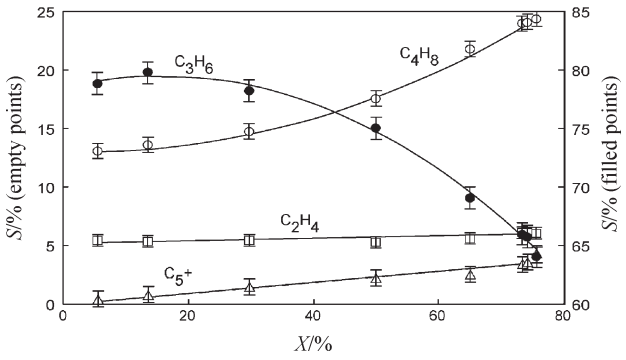

F i g . 5 – *Selectivity of 1-hexene catalytic cracking over EBK 13 catalyst at different conversions at 500 °C. Error bars reflect the expanded standard uncertainties at the 95 % level of confidence. Lines are fitted using polynomial regression to indicate data trends.*

Measuring kinetic data

A simple model reaction of cyclohexane dehydrogenation to benzene on the commercial palladium catalyst Cherox 40-00 (Chemopetrol Inc.) was chosen to demonstrate measurement of kinetic data and estimate kinetic parameters. The fraction of grinded catalyst tablets of particle diameter 0.4 – 0.8 mm was used for the catalyst bed (0.033 g) and was activated in the hydrogen stream at 350 °C. Experiments were carried out under two different pressure settings (184 and 300 kPa) and three different temperatures (T_w = 300, 350, 400 °C). While for some applications approximation of the reactor temperature with the temperature of its outer wall was sufficient, kinetic measurements are extremely sensitive to inaccurately measured temperature and thus the correction described in section 3.1 was essential for obtaining reliable data. A mixture of hydrogen and nitrogen Ψ_{H_2/N_2} = 1:10 (vol/vol) was used as the carrier gas. The conversion was measured for different contact times at each temperature and pressure.

We assumed that the catalyst deactivation played an insignificant role during the series of measurements. This assumption was validated by a test involving 25 experiments carried out under identical conditions to reveal any loss of catalytic activity during the time. Since no such loss was observed, a single catalyst sample was used for several experiments.

In order to evaluate the kinetic data correctly, the influence of the reverse reaction (hydrogenation of benzene) had to be determined. Therefore, a mixture of benzene and hydrogen was prepared (in gas phase) and injected into the reactor at 400 °C at the lowest possible carrier-gas flow rate. The observed conversion was far below 1 %, so that the reverse reaction could be easily neglected in the model design.

The mathematical model was based on the following assumptions, in addition to those given in previous section:

– Only a single catalyzed reaction occurs in the system – cyclohexane dehydrogenation,

– The pressure in the system is constant,

– The sample is introduced into the reactor as a rectangular pulse and passes through the reactor as a homogeneous cylindrical segment carried by the carrier-gas,

– Thermal effects of the reaction can be neglected, as there are inert layer and catalyst bed with thermal capacity high enough to offset the thermal effects of sample evaporation and reaction (this is valid only for samples of sufficiently low volume according to the analysis reported in the section 2.3),

– The flow rate increase due to the sample evaporation is negligible owing to the small volume of the injected sample and the presence of a buffer area before the catalyst bed. However, the effects of an increased amount during the reaction are significant and must be modelled.

The following chemical equation defines the chemistry of the model reaction:

$$\text{cyclohexane (A)} \rightarrow \text{benzene (B)} + 3\ \text{H}_2.$$

The power-law kinetics was used in the reactor balance (5), resulting in eq. (7)

$$\frac{\mathrm{d}c_\mathrm{A}}{\mathrm{d}(m_\mathrm{cat}/Q_\mathrm{pe})} = k\,p_\mathrm{A}^n \nu_\mathrm{A} = -k(x_\mathrm{A}\,p_\mathrm{r})^n = \\ = -k\left(\frac{1-X}{x+3X}\,p_\mathrm{r}\right)^n \tag{7}$$

where X is cyclohexane conversion and x_A is the mole fraction of cyclohexane in the feed. After expressing the concentration in terms of conversion it gives eq. (8), which was used for the regression analysis.

$$\frac{\mathrm{d}X}{\mathrm{d}(m_\mathrm{cat}/Q_\mathrm{pe})} = -k\left(\frac{1-X}{x+3X}\,p_\mathrm{r}\right)^n \frac{(1+3X)^2}{4}\,\frac{RT}{p_\mathrm{r}} \tag{8}$$

where k is the function of temperature according to Arrhenius eq. (9)

$$k = k_\mathrm{ref}\exp\left(\frac{E(T_\mathrm{r}-T_\mathrm{ref})}{R\,T_\mathrm{r}T_\mathrm{ref}}\right) \tag{9}$$

The reference temperature T_ref was chosen as the weighted average of temperatures of all experiments.

The kinetic model (eq. (8) and (9)) is able to describe conversion at the outlet of the reactor as a variable of contact time, reaction temperature, and pressure. The kinetic parameters of the model were estimated using ERA 3.0 software[16] (http://www.vscht.cz/kot/era/index.html). The results are available in Table 4. Fig. 6 shows the simulated conversion profiles by the contact time for different reaction temperatures T_r. Although the reaction temperature was determined for each experiment by the approach described in 3.1, the observed values of conversion are shown for three different levels of reactor wall temperature T_w for the sake of display simplicity. Since the temperatures T_r and T_w differed by up to 10 °C, depending on the carrier gas flow rate, the comparison is not quite accurate and the actual variance of data is a little lower than it can seem from the figure.

Table 4 – *Kinetic parameters of the power-law kinetic model of cyclohexane dehydrogenation on Pd catalyst*

Parameter	Value	Confidence limits 95 %
$k_{\mathrm{m,\ 348\ °C}}$, mol g_{cat}^{-1} min^{-1} MPa^{-n}	0.4	0.2 – 0.8
E, kJ mol^{-1}	22	15 – 30
n	2.2	1.9 – 2.5

While the power-law kinetic quantities are purely empirical owing to the character of the model, the apparent activation energy expresses the temperature sensitivity of the reaction. A Langmuir-

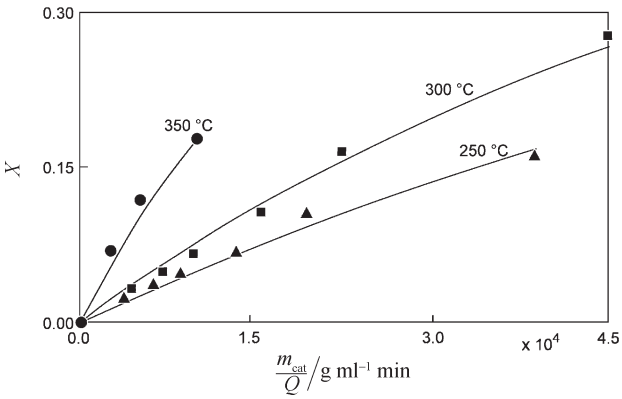

Fig. 6 – *Experimental data of cyclohexane dehydrogenation at different temperatures, compared to mathematical model simulations*

-Hinshelwood model was used to fit the experimental data as an alternative to the power-law and roughly the same residual sum of squares and estimate of apparent activation energy were obtained.

Conclusions

The laboratory results confirmed that the pulse micro-reactor technique is an efficient tool for screening tests in gaseous-phase reaction systems with or without the presence of a catalyst. It allows working with very small amounts of both the catalyst and the reaction substrate, yet it supplies experimental data efficiently. Therefore, using a multi-purpose Pyr-GC apparatus with a versatile analytical section in such a role may shorten the time needed for choosing the optimal catalyst, optimizing reaction conditions or even modelling the kinetics of a studied reaction system.

The developed mathematical model of homogeneous pulse carried by the carrier-gas in the plug-flow regime was validated on a well-known reaction system and its assumptions were justified. This model allows the experimental data from the pulse reactor to be treated as if they were measured in an ordinary plug-flow reactor, provided that the experimental arrangement remains in line with that presented in this paper.

The support provided for this study by the funds of the Czech Ministry of Education (MSM 6046137301) and the Institute of Chemical Technology (111/08/0016) is gratefully acknowledged.

Symbols

c – molar concentration, mol m^{-3}
d_p – particle diameter, mm
E – apparent activation energy, J mol^{-1}
k – rate coefficient, mol g^{-1} s^{-1} Pa^{-n}
n – reaction order
p – pressure, Pa
Q – feed rate, m^3 s^{-1}
r – reaction rate, mol g^{-1} s^{-1}
R – gas constant, Pa m^3 mol^{-1} K^{-1}
S – selectivity, %
T – temperature, K
V – volume, m^3
m_{cat} – mass of catalyst in the catalyst bed, g
w – mass fraction, %
X – conversion
x_i – mole fraction of compound i
ν – stoichiometric number
τ – residence time, s
Ψ – volume ratio
δ – thickness

Indices

cat – catalyst
e – equivalent value
n – carrier gas
p – pulse
r – in the reactor tube
s – mean value
w – reactor outer wall

References

1. *Christoffel, E. G.*, Laboratory Studies of Heterogeneous Catalytic Processes (Studies in Surface Science and Catalysis, Vol. 42), Elsevier Publ. Comp., Amsterdam, 1989.
2. *Igarashi, A., Ogino, Y.*, Appl. Catal. **2** (1982) 339.
3. *Campelo, J. M., Lafont, F., Marinas, J. M.*, Appl. Catal. A 170 (1998) 139.
4. *Aberuagba, F., Susu, A. A.*, Chem. Eng. Process. **38** (1999) 179.
5. *Aberuagba, F., Susu, A. A.*, Petroleum Sci. Technol. **20** (2002) 741.
6. *Aberuagba, F.*, React. Kinet. Catal. Lett. **70** (2000) 243.
7. *Susu, A. A., Ako, C. T.*, Appl. Catal. **16** (1985) 179.
8. *Lipiäinen, K., Hagelberg, P., Aittamaa, J., Eilos, I., Hiltunen, J., Niemi, V. M., Krause, A. O. I.*, Appl. Catal. A **183** (1999) 411.
9. *Ako, C. T., Susu, A. A.*, J. Chem. Tech. Biotechnol. **36** (1986) 519.
10. *Collyer, R., Larocca, M., de Lasa, H.*, Can. J. Chem. Eng. **67** (1989) 955.
11. *Christoffel, E. G., Surjo, I. T., Robschlager, K. H.*, Can. J. Chem. Eng. **58** (1980) 513.
12. *Ayo, D. B., Susu, A. A.*, Appl. Catal. **40** (1988) 1.
13. *Sica, A. M., Valles, E. M., Gigola, C. E.*, J. Catal. **51** (1978) 115.
14. *Ranzi E., Faravelli T., Gaffuri P., Garavaglia E., Goldaniga A.*, Ind. Eng. Chem. Res. **36** (1997) 3336.
15. *Bortonovsky, O., Sazama, P., Wichterlova, B.*, Appl. Catal. A **287** (2005) 203.
16. *Zamostny, P., Belohlav, Z.*, Comput. Chem. **23** (1999) 479.
17. *Zamostny, P., Belohlav, Z., Chládek, P.*, Investigation of Heterogeneously Catalysed Reactions in Micro-pulse Reactor in *Misek T.* (Ed.) Full texts of the 50th National Conference of Chemical and Process Engineering CHISA 2003 (CD-ROM), paper 111, pp 1–11, Orgit, Prague, 2003.